

## INVESTIGATION OF THERMAL DECOMPOSITION OF $\text{CrO}_x$ ( $x \geq 2.4$ )

*S. Łabuś, A. Małecki\* and R. Gajerski*

Stanisław Staszic University of Mining and Metallurgy, 30, Mickiewicz Avenue, 30-050 Kraków, Poland

(Received October 17, 2002; in revised form January 22, 2003)

### Abstract

The phase transitions and thermal effects occurring during annealing in air of material with general formula  $\text{CrO}_x$  ( $x \geq 2.4$ ) have been investigated. The investigations were performed with TG, DTA, DSC, EGA, XRD and other spectral techniques. The formation of an amorphous phase with average composition  $\text{Cr}_5\text{O}_{12}$  in the range 300–400°C has been observed. Further heating leads to partial loss of oxygen, simultaneous decay of  $\text{Cr}_2\text{O}_5$  and  $\text{CrO}_2$  phases and formation of nonstoichiometric  $\text{Cr}_2\text{O}_{3+x}$ . The distinct loss of mass is observed in the range 415–428°C, connected with evolving oxygen and small amount of nitric oxides. Thermal effects accompanying the mass changes depend on the mass of the sample. When the mass decreases, the transition from exothermic to endothermic effects is observed. This phenomenon can be explained as the competition between two processes: reconstruction of the crystalline lattice (endothermic effect) and recombination of the evolved atomic oxygen (exothermic effect).

**Keywords:** chromium nitrate nonahydrate, chromium oxides, phase transition, thermal decomposition

### Introduction

Chromium forms several oxides and oxide hydrates from which the most known and important are chromium(VI) oxide  $\text{CrO}_3$ , chromium(III) oxide  $\text{Cr}_2\text{O}_3$  and hydrated chromium dioxide  $\text{CrO}_2 \cdot n\text{H}_2\text{O}$ . In addition, among them there are many intermediate products with complex structures and properties, which depend on temperature, gaseous atmosphere, composition, humidity, pressure, etc. [1–3]. The superior properties of supported chromium oxide catalyst in alkane dehydrogenation are well-known, and  $\text{CrO}_x/\text{Al}_2\text{O}_3(\text{SiO}_2, \text{ZrO}_2)$  catalysts are widely used as the commercial one [4, 5]. Chromium(III) oxide is an important refractory material because of its high melting point (about 2300°C) and high-temperature oxidation resistance. As  $\text{Cr}_2\text{O}_3$  shows poor sinterability, only reactive powders for this purpose can be applicable [6, 7]. Ultrafine  $\text{Cr}_2\text{O}_3$  powders have a wide range of applications including green pigments, coating materials for thermal protection and wear resistance [8, 9]. Ther-

\* Author for correspondence: E-mail: malecki@uci.agh.edu.pl

mal decomposition of Cr-salts such as chromium(III) nitrate nonahydrate (CNN) is a common preparation method for  $\text{Cr}_2\text{O}_3$  and many other chromium compounds [7, 9–12, 15]. Depending on heating rate, final annealing temperature, type of gas atmosphere (inert, oxidising or reducing) etc., decomposition of this salt leads to different intermediate products with different physical properties and chemical composition. These conditions have also important influence on many properties of final decomposition products [7, 9–11, 13–15]. The products of the thermal decomposition of CNN obtained below  $250^\circ\text{C}$  are hygroscopic and therefore the investigation of their structure and properties is complicated [16–19].

Figure 1 presents TG and DTA curves of CNN heated with a rate of  $5^\circ\text{C min}^{-1}$  in flowing synthetic air atmosphere. The EGA for oxygen and nitric oxide were performed with the same rate of heating in pure helium atmosphere [19]. The TG curve between  $300\text{--}400^\circ\text{C}$  shows that the mass of decomposed sample is practically constant. The average mass loss of the initial CNN samples in this temperature range is 0.3% (22.8–23.1%). On the other hand, the Cr(VI) content of the samples between  $260\text{--}310^\circ\text{C}$  is in the range 7.6–8.2% which points to a molar ratio of  $\text{Cr}^{6+}/\text{Cr}^{3+} \approx 1.5$ , which is in agreement with total formula  $\text{Cr}_2(\text{CrO}_4)_3 \equiv \text{Cr}_5\text{O}_{12}$  [17, 18].

During heating the CNN sample dissolves in its hydration water at about  $50^\circ\text{C}$  (Fig. 1 – the first endothermic peak on DTA curve). Further heating causes gradual loss of water with simultaneous decomposition and liberation of gaseous products. The decomposition products have the form of tight spheres, in which residual gaseous products can be trapped [20, 21]. These phenomena lead to considerable enlargement of the product volume with respect to the initial sample and the thermal contact between the sample and crucible becomes poor. As a consequence, the DTA curve, particularly at its final part ( $410\text{--}430^\circ\text{C}$ ) can be indistinct and difficult for interpretation. It is possible to avoid this phenomenon by using under investigation

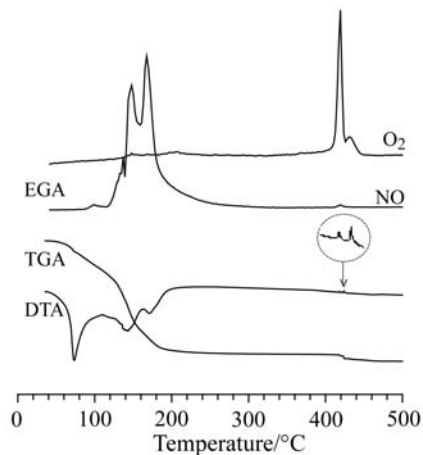


**Fig. 1** TG and DTA curves obtained by heating of  $\text{Cr}(\text{NO}_3)_3 \cdot 9\text{H}_2\text{O}$  at  $5^\circ\text{C min}^{-1}$  in synthetic air flow. The QMS analyses of selected gaseous product ( $\text{O}_2$ ,  $\text{NO}$ ) were performed in the stream of helium

some partially decomposed, not hygroscopic samples. Based on known investigation results [16, 17] it was stated that the best way was to employ the CNN decomposition product obtained at about  $300^\circ\text{C}$ . Samples collected at this temperature are stable and have a well-known chemical composition. They can be easily homogenized and ground to destruct their spherical structure. In addition, the mass of these samples receives about 23% of initial mass of the CNN. This fact allow to increase mass of decomposed samples for DTA/DSC (about 5x regarding to CNN) and precisely investigated thermal effects of the final stage of thermal decomposition.

The thermal effects and phase transitions occurred during heating for partially decomposed  $\text{Cr}(\text{NO}_3)_3 \cdot 9\text{H}_2\text{O}$  samples obtained at  $300^\circ\text{C}$ , in air, have been investigated in the present work.

## Experimental

### *Materials*

Chromium nitrate nonahydrate,  $\text{Cr}(\text{NO}_3)_3 \cdot 9\text{H}_2\text{O}$  was used for preparation as initial compound.  $\text{NaOH}$  and  $\text{K}_2\text{Cr}_2\text{O}_7$  were used for the spectral analysis. All reagents were analytical grade (POCh, Gliwice, Poland). The samples used for investigations were obtained from portion of CNN samples, in size of  $0.47 \pm 0.03$  g. The CNN samples were placed on a platinum plate and heated up to  $300^\circ\text{C}$  with a rate of  $5^\circ\text{C min}^{-1}$  in air. The volume of the furnace chamber was  $100 \text{ cm}^3$  and the airflow was  $100 \text{ cm}^3 \text{ min}^{-1}$  (controlled by flowmeter), which corresponds to 60 times per h of the atmosphere exchange. The decomposition process was programmed and controlled by computer. The flow of the synthetic dry air enables a quick removal of gaseous decomposition products such as water vapor and nitric oxides. The small portions of partially decomposed CNN samples were collected, carefully homogenized, ground and stored in the desiccator over anhydrous  $\text{CaCl}_2$ .

### *Thermal and mass spectroscopy (EGA) analyses*

The solid samples were analyzed using a SDT 2960 simultaneous DTA-TG and DSC 2010 apparatus (TA Instrument, USA) as well as EGA (Evolved Gas Analysis) by QMS (Balzers Instrument, Switzerland). The mass of the sample for TG/DTA investigations does not exceed 50 mg and for DSC – 15 mg. Both investigations were performed in synthetic airflow atmosphere with a heating rate of  $5^\circ\text{C min}^{-1}$ . The EGA investigation was realized in spectrally pure helium atmosphere.

### *X-ray diffractometry*

X-ray powder diffractometry (XRD) was carried out with the XRD7 Seifert diffractometer with Ni-filtered  $\text{CuK}\alpha$ . The diffractometer was operated with steps of  $0.01^\circ$  and a counting time of 10 s. Continuous intensity trace as a function of  $2\Theta$  was recorded. The obtained diffractograms were compared with ASTM standards to identify the phases.

### Spectral analysis

The samples of the decomposed CNN used to analyze the Cr(VI) content were obtained using a modified Paulik–Paulik–Erdey derivatograph (MOM, Hungary). Preparation and procedure were identical with those described in the preceding chapter. After the temperature set point was achieved, the heater was automatically stopped. The sample was then dissolved in 20 cm<sup>3</sup> of 20% NaOH and quantitatively transferred to a 100 cm<sup>3</sup> graduated flask.

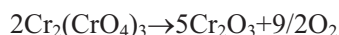
The samples prepared for investigation of Cr(VI) content were analyzed by means of the spectral method using an UV/VIS Philips spectrometer Model PU 8750 (England). 10 cm<sup>3</sup> of the alkaline solution were transferred to another 100 cm<sup>3</sup> graduated flask which was then filled to the scale mark. The solution was next filtrated through dense filter to remove the colloidal suspension of Cr(OH)<sub>3</sub>·*n*H<sub>2</sub>O. The calibration curve was prepared using aqueous solution containing adequate amounts of K<sub>2</sub>Cr<sub>2</sub>O<sub>7</sub>. The filtrates were analyzed using the wavenumbers 366 and 400 cm<sup>-1</sup>.

## Results and discussion

As shown in Fig. 1, heating of the sample in the range from 300 to about 415°C causes only little changes in mass. Above this temperature, in the range 415–430°C, a distinct loss of mass takes place. It is accompanied by evolving of oxygen and formation of the nonstoichiometric Cr<sub>2</sub>O<sub>3+x</sub> phase. In addition, EGA investigation [19] at this temperature range shows a small amount of nitric oxides (NO, NO<sub>2</sub>). These phenomena can be explained as thermal internal decomposition of solids [20, 21], connected with the reconstruction of their internal structure. Oxygen and chemisorbed (or trapped) nitric oxides are liberated during these processes. Further heating causes a gradual mass loss related to evolving of residual excess of oxygen (*x*→0), related mostly to decomposition of Cr<sub>2</sub>O<sub>5</sub> and CrO<sub>2</sub> phases and formation of stoichiometric chromium(III) oxide.

The quantitative analysis of chromium(VI) content in samples obtained during heating CNN in the temperature range of 260–310°C, shows that it decreases from 8.2 to 7.6±0.1%. Based on these results and on the assumption that the residue after decomposition consists of chromium(III) and chromium(VI) oxides mixtures, two limiting compositions: Cr<sub>5</sub>O<sub>12.2</sub> and Cr<sub>5</sub>O<sub>11.9</sub> can be calculated. For simplicity it was assumed that the oxide mixture obtained during heating CNN in air up to 300°C may be described by the general formula Cr<sub>5</sub>O<sub>12</sub>.

As it is revealed by Fig. 1, further heating of this product leads to its decomposition in accordance with the general reaction:



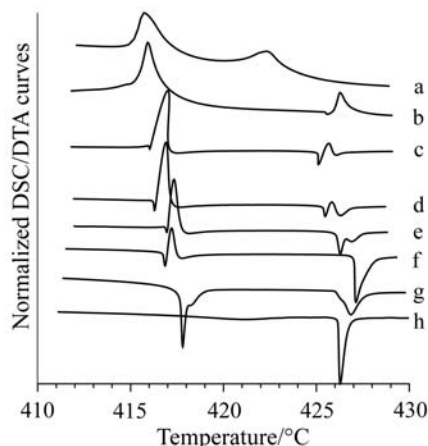
This process proceeds through several intermediate stages.

Figure 2 illustrates the normalized DTA curves of CNN (a) as well as DTA (b) and DSC curves (c–h) of Cr<sub>5</sub>O<sub>12</sub> samples heated in synthetic air. The masses of investigated samples were: a) 43.99 mg, b) 10.64 mg, c) 10.68 mg, d) 5.178 mg, e) 3.032 mg, f)

2.032 mg, g) 0.778 mg and h) 0.391 mg. Analysis of these results show that decomposition of CNN or  $\text{Cr}_5\text{O}_{12}$  to  $\text{Cr}_2\text{O}_3$  phase takes place in two main steps.

Figure 2a shows two exothermic DTA effects monitored during decomposition of CNN: the first with maximum at  $416^\circ\text{C}$  and the other at  $422^\circ\text{C}$ . This is interpreted so far to the thermal effects related to the crystalline formation of  $\alpha\text{-Cr}_2\text{O}_3$  from amorphous product [16].

Figure 2b presents the DTA curve of  $\text{Cr}_5\text{O}_{12}$ . Both samples have at  $410^\circ\text{C}$  practically the same mass, but adequate DTA curves are a little different. The temperature of the first exothermic effect is in good agreement with that of CNN but the other, at  $426^\circ\text{C}$ , has a small preceding endothermic effect. The next curves (Fig. 2c–g) were obtained of  $\text{Cr}_5\text{O}_{12}$  samples investigated with a DSC apparatus. The sample represented by Fig. 2c has, in relation to CNN, the same mass as described by 2b. As in Fig. 2b the other exothermic peak is preceded by an endothermic effect.



**Fig. 2** The normalized curves of a – DTA for CNN; b – DTA for  $\text{Cr}_5\text{O}_{12}$ ; c–h – DSC for  $\text{Cr}_5\text{O}_{12}$  samples

It is easy to notice that by moderate decrease of the sample mass the exothermic effects change into an endothermic one (Fig. 2d–g). For the sample with the smallest mass (Fig. 2h) the first peak practically disappeared, while the second is very sharp. These observations do not agree with literature data (only one exothermic effect). The following hypothesis can be formulated: in the range  $415\text{--}430^\circ\text{C}$  the structure arrangement process proceeds in two endothermic stages. The endothermic processes can be attributed to decomposition of the crystal lattice, their reconstruction and evolving the excess of atomic oxygen. The exothermic effects, which grow with the growth of sample mass, can be explained as recombination of atomic oxygen evolving from the sample. Decreasing of the sample mass increases diffusion of the atomic oxygen to the environment and causes that the exothermic reaction of recombination takes place outside the measurement place.

To confirm above hypothesis that the exothermic effects observed on DTA curves cause by recombination of atomic oxygen evolved during rebuilding of crystalline lattice

the following experiment was done. Samples with different mass of the parent material (CNN calcinated with rate of  $5^\circ\text{C min}^{-1}$ ,  $300^\circ\text{C}$ , air) were heated in DSC apparatus in different atmospheres with rate  $5^\circ\text{C min}^{-1}$ . The first part of these samples were placed in aluminum pans and tight covered by adequate lid for simplification of expected atomic oxygen recombination. Decomposition of these samples was done in the air atmosphere. The second part of the samples (in comparable sizes) were placed in open pans and heated in the stream of helium to reduce the partial pressure of oxygen and made recombination process more difficult. Results of these investigations are presented in Fig. 3.

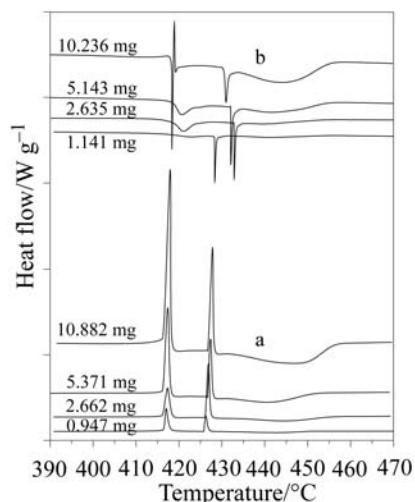


**Fig. 3** Curves of  $\text{Cr}_5\text{O}_{12}$  samples heated in different conditions: a – covered pans, air, b – open pans, helium. The distance between ticks on y-axis is equal to  $10 \text{ W g}^{-1}$

Part marked by (a) represents experimental DSC data for the samples heated in covered pans while part (b) shows analogous results for samples decomposed in open pans. The DSC curves of the samples (a) shows in the range  $410\text{--}430^\circ\text{C}$  two sharp, exothermic effects and one wide endothermic effect with minimum in the range  $440\text{--}450^\circ\text{C}$ . For the samples heated in helium (b) we have obtained quite different shapes of DSC curves. For sample with size close to 1 mg there was observed only one distinct endothermic effect ( $\sim 428^\circ\text{C}$ ). Increase of sample size (2.635 and 5.143 mg) leads to appearing two endothermic effects in the range  $415\text{--}435^\circ\text{C}$ . Further increase sample size cause difficulties in atomic oxygen evolution and made easier recombination in the sample volume. The DSC curve obtained for largest sample (10.236 mg) reveal vs. an endothermic effect background the exothermic one.

In order to investigate the influence of temperature on the structural changes of  $\text{Cr}_5\text{O}_{12}$ , X-ray powder diffractograms of samples obtained at  $300$ ,  $400$ ,  $420^\circ\text{C}$  (after first exothermic peak – Fig. 2b),  $430^\circ\text{C}$  (after second peak),  $500$ ,  $600$  and  $700^\circ\text{C}$  were performed. The examined samples were prepared by heating  $\text{Cr}_5\text{O}_{12}$  in the DTA/TG equipment in air with a rate of  $5^\circ\text{C min}^{-1}$ . Results of these investigations are presented in Fig. 4.

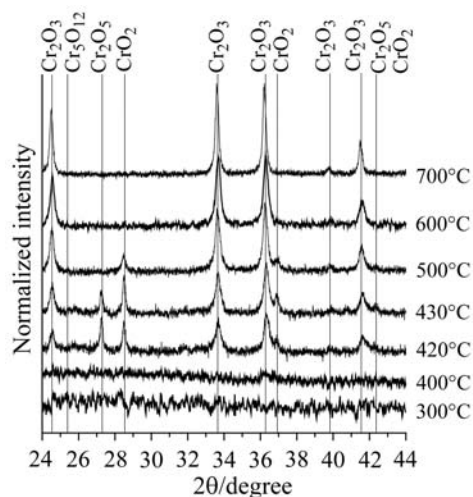


Fig. 4 XRD patterns of  $\text{Cr}_5\text{O}_{12}$  samples heated to the different temperatures in air

XRD patterns show that the initial sample (CNN heated up to  $300^\circ\text{C}$ ) as well as the sample from  $400^\circ\text{C}$  are completely amorphous. Taking into account the analytical results, the sample can be formally described by the hypothetical formula  $\text{Cr}_5\text{O}_{12}$ . However, on the X-ray diffractogram (Fig. 4) no crystalline  $\text{Cr}_5\text{O}_{12}$  phase were observed. The diffraction patterns for samples obtained at temperatures of 420 and  $430^\circ\text{C}$  display peaks belonging to  $\text{Cr}_2\text{O}_5$ ,  $\text{CrO}_2$  and  $\text{Cr}_2\text{O}_3$ . At 500 and  $600^\circ\text{C}$  two phases were observed:  $\text{Cr}_2\text{O}_3$  and  $\text{CrO}_2$  (traces). The diffractogram for sample obtained at  $700^\circ\text{C}$  show  $\alpha\text{-Cr}_2\text{O}_3$  only. Obtained results are in good agreement with results, reported by Maciejewski *et al.* [10].

## Conclusions

- Thermal decomposition of the CNN in dry air atmosphere leads to the formation of different oxides with variable contents of chromium(VI). The maximum concentrations of the Cr(VI) appear in temperature range of  $260\text{--}310^\circ\text{C}$ . It can be stated that there exist oxide mixtures, which can be described by the formula  $\text{Cr}_5\text{O}_{12}$ .
- Thermal decomposition above  $420^\circ\text{C}$  of the amorphous oxide mixtures with general formula  $\text{Cr}_5\text{O}_{12}$ , causes the formation of crystalline phases:  $\text{Cr}_2\text{O}_5$ ,  $\text{CrO}_2$  and  $\text{Cr}_2\text{O}_3$ . When the final temperature increases, the amount of  $\text{Cr}_2\text{O}_5$  and  $\text{CrO}_2$  gradually decay. At  $700^\circ\text{C}$  only individual crystallites of  $\alpha\text{-Cr}_2\text{O}_3$  remain.
- Phase transformations in the temperature range  $415\text{--}428^\circ\text{C}$  proceed in two stages. Both stages are connected with two main competitive effects: lattice reconstruction (endothermic) and atomic oxygen recombination (exothermic).
- The liberation of nitric oxide over  $400^\circ\text{C}$  can be explained as breaking of the  $\text{CrO}_x$  framework in which  $\text{NO}_x$  were chemisorbed or trapped.

The financial support of Polish Committee for Scientific Research, Project No. 11.11.160.94, is acknowledged.

## References

- 1 T. V. Rode, Oxygen compounds of chromium catalysts, Izd. Akad. Nauk SSSR, Moscow 1962, Macmillan, London (1965).
- 2 R. Richelmi and M. Laffitte, C. R. Acad. Sci. Paris, 265 (1967) 541.
- 3 O. Fukunaga and S. Saito, J. Am. Chem. Soc., 51 (1968) 362.
- 4 C. P. Poole and D. S. Maciver, Adv. Catal., 17 (1967) 223.
- 5 B. M. Weckhuysen and R. A. Schoonheydt, Catal. Today, 51 (1999) 223.
- 6 P. D. Ownby and G. E. Jungquist, J. Am. Ceram. Soc., 55 (1972) 433.
- 7 T. Komeda, Y. Fukumoto, M. Yoshinaka, K. Hirota and O. Yamaguchi, Mat. Res. Bull., 31 (1996) 965.
- 8 T. Tsuzuki and P. G. McCormick, Acta Mater., 48 (2000) 2795.
- 9 M. Ocaña, J. Europ. Ceram. Soc., 21 (2001) 931.
- 10 M. Maciejewski, K. Koehler, H. Schneider and A. Baiker, J. Solid State Chem., 119 (1995) 13.
- 11 A. Małecki, B. Małecka, R. Gajerski and S. Łabuś, J. Therm. Anal. Cal., 72 (2003) 135.
- 12 P. Moriceau, B. Grzybowska, L. Gengembre and Y. Barbaux, Appl. Catal., 199 (2000) 73.
- 13 Z. V. Marinković, L. Mančić, R. Marić and O. Milošević, J. Eu. Ceram. Soc., 21 (2001) 2051.
- 14 I. Takahara, W.-C. Chang, N. Mimura and M. Saito, Catal. Today, 45 (1998) 55.
- 15 D. D. Berger, I. Jitaru, N. Stanica, R. Perego and J. Schoonman, J. Mater. Synth. & Proces., 9 (2001) 137.
- 16 L. Gubrynowicz and T. Strömich, Thermochim. Acta, 115 (1987) 137.
- 17 S. Łabuś, VII Conference of Calorimetry and Thermal Analysis, Zakopane, Poland, Abstracts 1997, p. 309.
- 18 N. E. Fouad, S. A. Halawy, M. A. Mohamed and M. I. Zaki, Thermochim. Acta, 329 (1999) 23.
- 19 A. Małecki, Ceramika-Materiały Ogniotrwałe, 4 (2000) 123.
- 20 J. Stoch, J. Thermal Anal., 37 (1991) 1415.
- 21 J. Stoch, Thermochim. Acta, 203 (1992) 259.